Lens Integrated Based Optical Tomography System: The Selection of Optical Sensor and Projection Arrangement

Mohd Fahajumi Jumaah[1], Ruzairi Abdul Rahim[1*], Siti Zarini Mohd Muji[2], Nasarudin Ahmad[1], Khairul Hamimah Abas[1], Ahmad Ridwan Wahap[1]. Jaysuman Pusppanathan[7], Mohod Hafiz Fazalul Rahiman[3], Juliza Jamaluddin[6], Suzanna Ridzuan Aw[5], Yasmin Abdul Wahab[4]

[1]*Process Tomography Research Group, School of Electrical Engineering, Faculty Engineering, Universiti Teknologi Malaysia, 81310 UTM, Malaysia.*
[2]*Faculti of Electrical & Electronic engineering, Universiti tun Hussein Onn Malaysia, Batu Pahat*
[3] *Centre of Excellence for Advanced Sensor Technology, School of Mechatronic Engineering, Universiti Malaysia Perlis, Arau 01000, Malaysia*
[4]*Faculty of Electrical and Electronic Engineering, Universiti Malaysia Pahang, 26600 Pekan, Pahang*
[5]*Faculty of Electrical & Automation Engineering Technology, TATiUC, Jalan Panchor, Telok Kalong, Kemaman, Terengganu, 24000, Malaysia*
[6] *Faculty of Engineering and Built Environment, Electronic Engineering Department, Universiti Sains Islam Malaysia, Nilai 71800, Negri Sembilan*
[7]*Sports Innovation & Technology Centre (SiTC), Institute of Human Centered Engineering (iHumen), Faculty of Engineering, Universiti Teknologi Malaysia 81310 Skudai Johor.*

Corresponding author email: ruzairi@fke.utm.my

Abstract

This research investigates the methods of implementing switch mode parallel beam projection technique into an optical tomography instrument, and observes the effects of lens in optical system tomography. This paper discusses the selection of optical sensors and its projection techniques.

Keywords: optical tomography, lens, projections.

1.0 Introduction

The selection of the optical sensors is crucial in the first stage of tomography. To ascertain that the system will operate efficiently, a comprehensive selection of the sensors must be performed. The selection of the sensors is influenced by the projection arrangement of the selected optical sensors. These are parallel beam mode and fan beam mode.

For parallel beam mode, the sensors have a narrow angle beam while fan beam mode uses wide angle beam. Both projections; parallel and fan beam mode have their own advantages and disadvantages. The main difference between parallel beam and fan beam modes is depicted in Figure 1.

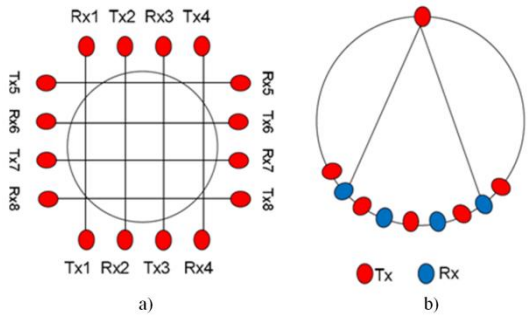

Figure 1: a) Parallel beam projection, b) fan beam projection

In parallel beam projection, the sensor is arranged as one transmitter to one receiver. Meanwhile, for fan beam mode, one transmitter covers several receivers. As shown in Figure 1(a), the parallel beam projection is simple and easy to implement. This is because all transmitters and receivers will be 'ON' at the same time and no switching control is needed on the transmitter part. However, this simple construction has poor coverage where the line of light is straight and only certain parts will be covered. Blank spots or parts that cannot be detected will directly affect the tomogram result.

For fan beam mode as shown in Figure 1 (b), the detection coverage is 100% of the pipe cross section. However, the vital drawback of this mode is that the switching process of the detectors from one transmitter to another transmitter until the entire transmitter array finished performing the scanning, critically delays the detection period.

2.0 Optical Sensor and projection Arrangements

Investigations were carried out to identify the best detection for optical tomography by coupling different sensor methods to different beam modes. The investigated groups are listed as below:

a) Fiber optic and parallel beam mode [18, 22]
b) LED and fan beam mode [3, 16, 15]
c) Infrared and parallel beam mode [10, 19, 13, 14, 19]
d) Infrared and fan beam mode [17],
e) Laser and parallel beam mode [7,8],
f) laser And fan beam mod e [16, 24] and
g) Dual mode [18, 25].

2.1 Fiber Optic and Parallel Mode

The preparation of fiber optics in optical tomography was a challenging job as incorrect cutting procedures will cause fault measurement. Therefore, careful setup of the system is necessary. Optical tomography using fiber optics for measuring different materials have be reported [18, 22].

Fiber optic as a sensor tool is used [22]. The diameter of the pipe in his research was 81mm. The light source was a single quartz halogen that provided a large beam area. It produced good illumination for all the optical transmitter fibers, which were arranged in a bundle. The receiver fiber converted the signals into electrical signals by PIN diodes. Although only 16 pairs of fiber optic transmitters and receivers were used and arranged in two projections, it is still capable of producing the concentration profile and tomographic images successfully. Besides that, this research also performs well in getting the result for particle size distribution. The assumption used to obtain the results is to ignore the effect of scattering and diffraction of light [22]. One drawback of fiber optics is that the transmitters and receivers need to be aligned accurately. Otherwise, the sensors will produce incorrect readings and this can greatly reduce the accuracy of the system. Another problem arises would be related to the light collimating issue where the arrangement of transmitters and receivers in a group might create a problem since the possibility of overlapping is higher between adjacent receivers. This results in intensity loss. Although there are negative effects, fiber optics provide the opportunity to design sensors with a wider signal bandwidth which enables measurements of higher speed flowing particles. Some improvements in image reconstruction algorithm are needed to obtain a better image as well. Apart from that, the CPU speed and data acquisition need to be improved to make the system more reliable.

They has some researchers put in some enhancements in optical tomography [18]. The fiber optics used in his experiment were arranged in two planes, which was different from Abdul Rahim who used only one plane [22]. Each plane consists of two rectilinear and two orthogonal projections. For orthogonal, 8 by 8 sensors were implemented while for rectilinear, 11 x 11 sensors were used. The total numbers of transmitter sensors in one plane were 38. The unique feature was the implementation of four 35cm projectors as light source and light guide. This research ignores the scattering effects and also neglects the fiber cladding as it is assumed thin in comparison to the central fiber. As a result, small bubbles in diameter of 1-10 mm and a volumetric flow rate up to 1 l/min can be detected using optical

tomography. The optical tomography is sensitive to large bubbles in water of diameter 15-20 mm and volumetric flow rates up to 3 l/min [18]. This modification produces a result with higher resolution than the previous research done by Abdul Rahim due to the increment in the number of sensors [22]. However, the arrangement of the receivers and transmitters in a group will result in an overlapping beam for the receivers. Different forms of filtering techniques in the reconstruction algorithm should also be investigated in order to produce better results.

2.2 LED and Fan Beam Mode

The best characteristics of LED are the minimal power drawn, its longevity and its cost compared to many other sensors [24,26]. LED has a slow rise time and fall time, but it can still be used in the optical tomography system as was demonstrated by [9, 15]. They proved that LED is feasible for optical tomography applications.

In 2002 the LED is used as a source of light and PIN photodiode as a receiver, both with diameters of 2.94 mm [15]. The sensors were arranged in a fan beam projection technique and the total numbers of sensors installed are 16 pairs as shown in Figure 2. The fan beam method exploits a larger emission angle of the source that was feasible to be sent to all the receivers and the emission power is uniform along with the projection. There are a few assumptions that had been made which include:

i) Light scattering and beam divergence effects are neglected.
ii) The attenuation factor for air is assumed to be zero while the attenuation factor for solid particle is assumed to be one. All incident lights on the solid surface are fully absorbed.
iii) Single projection resulted in 16 light beams from the emitter towards the photodiodes and each of the light beams possesses a different width, depending on the sensor geometry and projection angle.

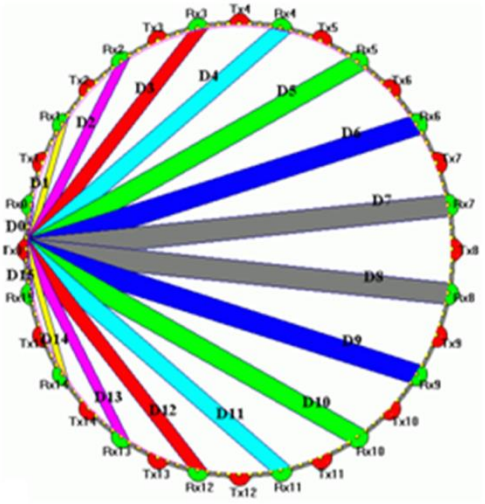

Figure 2 : Sensor arrangement used 16 pairs of sensor

Red LED are chose as the source of a transmitter and in parallel with the light that will be detected by the photo valve at the other side [9]. They used a rotary working table for the experiment setup to get the complete projection for the object. In this project, they employed one of the optical scattering methods, which is a light extinction method but ignored the diffraction effect that is formed by the edged of the particles. Sand in a diameter of 120 μm was dropped through a funnel and the flow velocity was observed to be dependent on the controlled funnel. Thus, by changing the velocity, different optical signal would be obtained. From the experiment, a random fluctuation signal was produced, where it was related to the light decrement. As the light decreased, more particles were shown to be passing through, which blocked the light source which is an indication of a higher mass concentration.

2.3 Infrared Led and Parallel Beam Mode

Infrared LED has a characteristic of invisible to human eyes, and it is more difficult to handle compared to LED as it was hard to check for alignment. However, this type of sensing element is recommended since its wavelength is outside of visible light; therefore, the interruption of day light can be avoided. The researchers used infrared in parallel projection for optical tomography [12,13,14].

The infrared LED from the TEMIC Semiconductor model TSUS4300 that had a wavelength in the range of 900 to 1000 nm, whereas the peak of wavelength was at 950 nm [12]. Thus, the optical tomography sensor designed is indisputably unaffected by the visible light source from the surrounding environment that will result in error during the

measurement process. The feature of a small angle of half intensity, which was 16 degree, is the main criteria to take into account because they implement parallel beam mode in their project. For the receiver, Pang had chosen phototransistor instead of photodiode due to the compatibility of the phototransistor model, TEFT4300 to the infrared LED [90]. The advantage of phototransistor was that the starting wavelength of phototransistor was about 875nm whicht was well away from the visible light's boundary, 700nm. Most photodiodes available in the market are sensitive to visible light. It has a physical size of 3 mm in diameter, peak of wavelength is 925 nm, and angle of half sensitivity was 30 degree and less costly.

For the experiment purposes, plastic pellets also being used, which look like a small cylinder in the dimension of 2 x 2 x 3 mm to be imaged [12]. It will be tested to observe the difference of concentration profile in four kinds of a regime (full flow, three-quarter flow, half flow and quarter flow). To measure the mass flow rate, three other regimes were set up with a diameter of 4.5 cm, 4 cm and 3.5 cm. The dropping distance is 16 cm and 56 cm. The smaller the drop distance, it will produce higher concentration.

For the projection technique, Pang implemented two orthogonal and two rectilinear projections per layer (16 pairs for one orthogonal projection and 23 pairs for one rectilinear projection) as shown in Figure 3 [12].

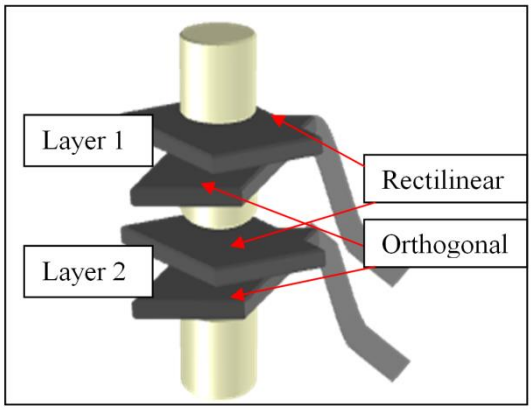

Figure 3 : Two-layer of projection [12]

This projection method has doubled the amount that Ibrahim in (2000) did and this has enhanced the resolution [11]. The two-plane arrangement (upstream and downstream) may cause misalignment of objects that passed through from an upper stream to downstream because they cannot be projected in the same layer. This will affect the velocity parameter in this system. Therefore, the distance between two orthogonal and two rectilinear needs to be reduced where the better solution is to make all the projection in the same layer. Nevertheless, this type of projection can successfully determine the online mass flow rate without involving

any calibration constant. There are still some improvements that can be done in this research to improve the time to get the mass flow rate measurement and the tomogram image. It is suggested to use a higher sampling rate of the DAS card rather than DAS-1802HC. Another alternative is to design a simple and cheaper data acquisition system using, for example, Ethernet, USB, DSP and FPGA technologies. Furthermore, the computational issue in this project should be addressed, where; it involved four powerful personal computers and a network hub in order to implement a data distribution system. This would result in a large and non-portable system.

Goh identified Pang's problem and applied a single plane for the system as shown in Figure 4 [12,14]. It has improved the system because all measurements for orthogonal and rectilinear projections were done in the same layer. Therefore, the measurement is more precise than Pang's technique. The uses of Ethernet-based data acquisitions were beneficial in assisting a higher data transfer in the solids flow meter system and develop long-distance monitoring unit. However, this work has a weakness in terms of mass flow rate measurement where a calibration is needed every time new materials are to be tested. Other than that, the circuit became bulky and crowded which could easily cause a short circuit. The distance between emitters and receivers was increased which has directly affected the intensity of the light and also the image to be displayed. The sensors are utilized from Agilent, HSDL 4420 as an emitter and HSDL 5420 as a receiver (Ø = 2.54 mm). Two orthogonal and two rectilinear projections were implemented [92]. The configurations of the sensors were 16 pairs for each orthogonal projection and 16 pairs for each rectilinear projection.

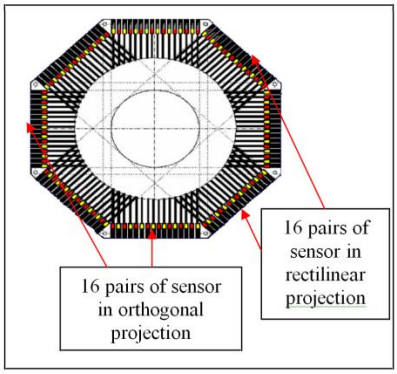

Figure 4: One layer of sensor jig [14]

These sensors have good performance in many ways. Firstly, the sensors operated in the 875 nm region which is far from visible light (700 nm). Secondly, it can operate with a narrow beam area where its half angle of the full radiation angle is 12 degrees. The selection of a receiver matched the transmitter in terms of spectral, peak sensitivity, and size. Goh

selected photodiode as a receiver for its faster response in nanosecond in comparison to phototransistor (in μs) [92]. It also discovered that at a concentration percentage of 80%, the flow saturates at the flow rate of $752gs^{-1}$ [14]. At higher solids concentration, the mean free path is short and the randomness of particle movement is dampened by collisions. A test is performed to investigate the overall timing diagram for the developed tomography system. This is done by setting a resolution of 128 x 128 pixels for image reconstruction using the interpolation technique in the DSBP algorithm. The image reconstruction was processed in 2.70 ms and it gave 370 frames per second (fps), which is quite good because the time to complete reconstructing one cross-sectional image is only 2.70ms. Goh used some assumptions in her research, where the attenuation factor for air is assumed safe to be zero while the attenuation factor for solid particle is supposed to be one [14]. In other words, all incident lights on the surface of a solid particle are fully absorbed. The light scattering and beam divergence effecst are ignored. From the Ethernet link speed analysis, the data transfer rate is restricted by Rabbit microprocessor 21 MHz CPU speed. It is proposed to use the DSP processor, which can operate at the CPU speed up to 400 Mhz.

Chiam used the same type of sensors and projection method as Pang [12,13]. Enhancement in the data acquisition unit was done using Hybrid DSP, which is the combination of microcontroller and DSP chip. Standard data acquisition card (DAQ) or modules with similar capabilities would have cost more than RM10000.00 whereas the developed system only require less than RM2000.00 for the DSP chip, electronic components and PCB fabrication. His research results and findings are proven to be better than Pang's discovery. Mass flow rate measurement was produced in 430 ms processing time. The implementation of the new hybrid image reconstruction has increased the quality by 12.5% because the new algorithm reduces the possible errors in image reconstruction of the arc-shaped object. The processing time to obtain flow velocity is 12 times faster by using sensor-to-sensor cross-correlation in the frequency domain compared to pixel to pixel cross-correlation in time domain. An assumption for using cross-correlation technique for flow velocity measurement is that the arrangement of particles flowing through the downstream sensor layer is a time-delayed replica of the upstream sensor layer. There are some enhancements that can be done in this project where the application of a multi-processor based embedded system can further improve the performance of the overall system. Pipelining technology used in CPU design or parallel processing method can be implemented to increase the throughput.

Infrared LED and photo detector managed to produce the tomogram for bubble investigation [10]. They implemented infrared emitters and detectors to exploit the optical characteristic. Two types of orthogonal arrangement were investigated, which was the 8 × 8 and 16 × 16 configurations. Small planoconvex glass lens with dimension 5 mm in diameter and 8.7 mm back focal length was used to acquire a beam from the LED. Obviously, by increasing the number of sensors to 16 x 16, the resolution would increase, where the configuration of 16 transducers per projection was the optimum hardware design till the present. Therefore, further improvements in resolution needs to attach more projections that require a new algorithm. In this technique, smaller objects that are below 5 mm in diameter cannot be detected. Accordingly, to overcome this drawback, more sensors should be arranged to make the gap between the light beam decreases as much as possible.

2.4 Infrared Led and Fan Beam Mode

The fan beam mode applies by using infrared emitters coupled with fiber optics [17]. The type of infrared was SFH484-2 with wavelength peak at 880 nm and a small radiation angle of 16 degrees. The small radiation angle was vital as the emitting area needed for the infrared to be coupled with the fiber optics was small and narrow. As for the receiver, photodiode SFH213-FA was used. Two assumptions had been made in his project. Firstly, all incident lights on the surface of the solid materials are fully absorbed by the object. Secondly, the effect of light diffractions and scatterings are ignored because the primary effect is the attenuation of optical energy by particles intercepting the beam. Leong increase the number of sensor pairs to 32 in contradiction to Chan that only used 16 pairs. Figure 5 shows the sensor arrangement [15,17].

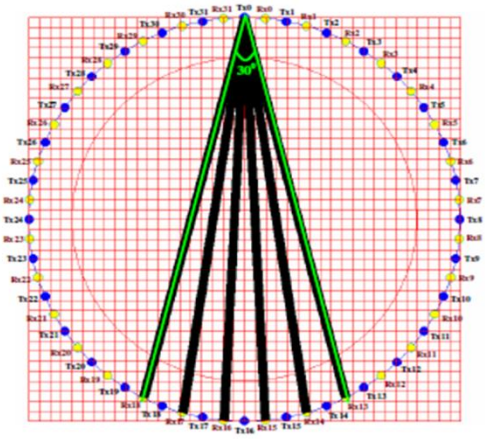

Figure 5 : Sensor arrangement using 32 pairs of sensor

Since the physical size of the fiber is small, the effort to double the number of sensors seems to be a very effective technique. However, there is a computational issue that should be resolved first. The present data acquisition card needs the ISA slot for communication. The ISA slot feature is currently not available in the latest generation of Pentium IV computers. It is suggested that the new model, Keithley DAS1802HC, that communicates using the PCI slot should be used. The PCI slot is attainable in many computers and this will help in obtaining a faster image processing rate since the speed of the computer processors in the market can achieve up to 2.4 GHz or higher. As an alternative, it is also proposed that specific data acquisition system for process tomography should use Ethernet, USB, or FPGA technologies for cheaper communication.

2.6 Laser and Parallel Beam Mode

Laser is a type of coherent light output, and it has high speed in fall and rise time compared to LED and infrared. The emitting area of a laser diode is smaller in comparison to LED and infrared in the factor of 30000. However, laser is partially nonlinear and varies with the temperature, similar to LED and infrared. In terms of safety, laser diodes are more dangerous and harmful to our eyes.

On the other hand, researchers has proposed a research where the objectives are to produce a cross sectional images of a flame [14,15]. This is accomplished by using the laser Neon as the source of light, where it illuminates the fiber optic causing the light to flow through it. Eight pairs of transmitter and receivers were utilized to be applied for two orthogonal projections. The use of fiber optic could perform well since it produced perfect collimation. The developed system had been tested by locating a cylinder object with a diameter of 3 mm in the pipe with an image plane [7]. For flame testing, two models were tested; the half and full open. The study showed that, for half open the concentration was higher than the full open. This is because the flame intensity was higher and not because of the larger size of the flame. In this project, the flame image generated from the image results is not shown in an accurate manner.

2.7 Laser and Fan Beam Mode

Chen adopted the medical tomography technique (optical computed tomography) in the process industrial research [16]. The use of near infrared laser diode was assumed to have moderate water absorption. This was suitable for the parameter measurement of two phase

flows. The advantages of sensor selection are the compact structure and also its high frequency. The projection in this research was based on parallel scanning and serial receiving which can avoid the disturbance of optical reflection and refraction effect. There are six NIR diode lasers as a transmitter and 48 NIR diode sensors worked as receivers where the wavelength for diode laser was 780 nm, beam diameter equal to 1 mm and the power output was 10 mW. The scan sector for the emitter contained 24 receiver sensors. Therefore; one scan cycle collects 144 projection data. The resolution of the system could easily be changed from the mm level to the μm level and it was done by changing the laser beam diameter and sensor density; consequently, increasing the flexibility of the measurement. The researchers concluded that the more emitter involves, the more projections can be produced and this can directly increase the resolution of the image. There are three factors that can influence the system response speed, the speed of scan of the emitter, the speed responds of the receiver and the operation speed of the image reconstruction algorithm. Since the system covered all these factors, the system clearly had a high respond speed.

Zheng did a research on optical tomography to measure concentration profile and mass flow rate [21]. The system consists of an array of laser diode sources and photodiode as a detector. They manipulated fan shape beam projection and divided three structures of an array which consists of 4 sources 15 beams, 8 sources 15 beams, and 15 sources 15 beams. The outcome showed that 15 light source and 15 beams produced the smallest Space Image Evaluating (SIE) which was 7.67%. SIE was based on error theory in science measurement where the grey values in original images are subtracted from reconstructed image. The result was then divided to grey values of the original images. The computational time was higher because they used a large number of sensors and therefore more time was needed to rotate each of the sources. The experiment aimed to reconstruct the concentration distribution and validate the relationship between the optical attenuation (projection sum) and the mass flow rate. The calibrated the measurement coefficient K at different screw feeder speed are already done [21]. From there, the relationship between mass flow rate and projection sum was linear. There are a few assumptions for this research where, the particle velocity is constant and measuring environment, physical and chemical features of the particles are kept invariable, so the calibration coefficient is approximately a constant.

Zhang in 2005 enhanced the works done by Chen in 2005 [16, 20]. New approach was implemented which was based on Terahertz process tomography. Near infrared (NIR) prototype system has become the simulator of terahertz tomography because the wavelength

of NIR is near to Terahertz's. All the projections used were the same with Chen in 2005 [16]. The absorption effect was tested on a circle diameter of 50 mm. Three opaque cylinders with diameter 3 mm, 5 mm and 7 mm were used. This arrangement was the same as Chen's studies. Terahertz has a characteristic of quasi optic features like visible and infrared too. Therefore quasi optic scan model can be used in Terahertz system, and it was more stable and simpler in comparison to X-ray process tomography. The set of Terahertz sources and receivers were distributed uniformly around the pipe and the amount of sensors was depending on the pipe diameter. The static scan mode used in their research could produce an appropriate respond of speed.

2.5.7 Dual Mode Tomography

Rasif in 2009 and Rzasa in 2009 in their research both used optical fan beam projection combined with electrical capacitance tomography [18, 27]. However, due to the difference in the vessel conditions, the optical projection differed from each other. Rasif focused on vertical while Rzasa in horizontal measurement [18, 27]. Rasif only used single projection while Rzasa used 5 projections to cover the cross sectional area inside the vessel. Rasif used 16 pairs of optical sensors, and the type of sensors is similar with Chan in 2002 [18,27], that has 5 mm in diameter. Rzasa used 64 phototransistors as a detector with five light sources from the 55 W bulb [114]. Rzasa designed five planes with 7 mm distance from each other while Rasif uses single plane [18,27]. Both researchers agreed the joining images of optical and electrical capacitance tomography will give a better resolution in final image reconstruction.

2.6 Lens

The application of the lens is more to capture an image from a camera or oscilloscope [28]. The application can be applied to the binoculars concept. The lens can convert and make the light go through in a way that is easy to manage and thus make the output after the lens better than that before the light goes through the lens [29]. Figure 6 shows the basic application of the lens base on the theory of lens.

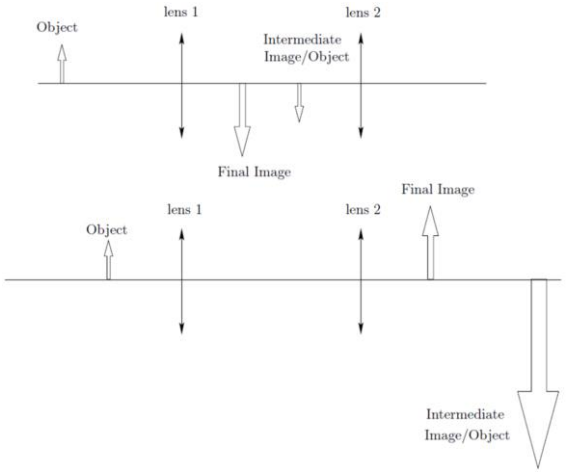

Figure 6 : Lens application

Figure 7 shows the basic application when testing the effect of the lens. Based on Figure 7, the testing included the projection, focal point, refractive index, and others. By using the method of testing, results can also be calculated to check the properties of materials that may be used to build the lens. Based on a study, the laser is used as a reference point which is used in flight scanning research. Normally flight research uses a laser as a source to detect objects high above the ground [30].

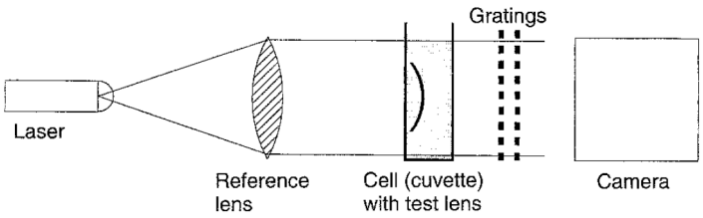

Figure 7 : Basic lens testing

Based on the study of lenses, lenses are already applied in contact lenses and a lot of research has already been done to check the effect of contact lenses on human vision. Normally a contact lens is built by using a convex lens[119]. The patent of the contact lens is adapted to the eye shape [32,33].

$$D = \frac{1}{f_{\text{test}}} = \frac{\Delta_z}{f^2_{\text{ref}}} \quad (1)$$

Equation (1) is used to calculate the power of lens which is D is the power of the cuvette-contact lens combination, f_{test} is its back focal length, f_{ref} is the focal length of the reference lens and Δz is the distance.

$$t(r) = t_0 - \frac{r^2 P}{2(n-1)} \quad (2)$$

The equation (2) is used to calculate radial distance, when t_o be Centre thickness in meters and P is the power of the lens [33]. The value obtained from the equation is only estimated and it can be used in the real world but is not very accurate [33].

In the industry environment and the real world, there are many types and names of lenses, but the function of a lens is to make the output either focus or diverge depending on the output needed. The effect of lenses in applications, for example for the human eye, camera lenses, biomedical imaging, and optical lithography, the lens makes the component more effective and efficient compared with applications without a lens it makes the quality of result much better by applying the lens [6, 34, 35]. A study also demonstrated that dust can make the reading captured by a sensor inaccurate [36]. Therefore, every material can be used to make a lens, but the output of the lens must be considered to make the lens more suitable for the situation [25,37]. The material must have transparent properties so that light can penetrate the material, for example protein, plastic, glass, and so on [35, 37, 38]. The concentration of material can also make the output of the lens (convex lens) change and it may be more focused or not depending on the refractive index of the material itself [28,30, 33,34, 34,35, 37]. Normally, when a convex lens is applied, there is a focal point when the light penetrates into the lens. The figure shows an example of a focal point [31]. A study showed that the refractive index can be controlled when the manufacturer carries out the correct process during the formation of the lens, but it also depends on the material itself [30, 38]. Based on that process, the lenses must be examined one by one to get the same refractive index for each lens used in the tomography system.

The material would become a phantom and causes an effect when penetration of light is taking place. The density of the phantom means that light can penetrate it [36]. H2O (water) can also refract light when the light penetrates it. Figure 8 shows that the effect of the refractive index happens in the real world and can be easily found in real life [28,29]. In the real world a straw is a straight object but when it enters the water it will be refracted, as shown in the figure.

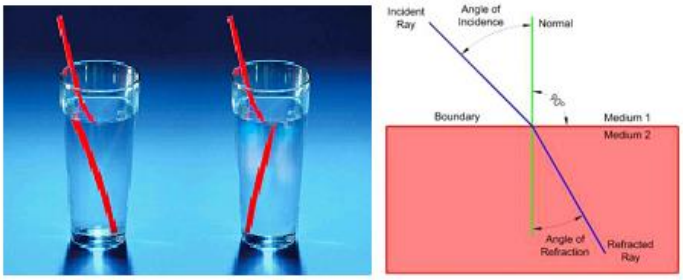

Figure 8 : Effect of refract

Table 1 shows that the lens's focal length and the object's distance from it determine the image type. According to the table, the only way to form an upright enlarged image is to place an object within the focal length of a converging lens.

Table 1: The lens's focal length and the object distance

Focal Length f	Object Distance s	Image Distance s'	Image Orientation	Image SIze
Converging Lens $f > 0$	$s < f$	$s' < 0$, virtual	upright	enlarged
Converging Lens $f > 0$	$f < s < 2f$	$2f < s' < \infty$, real	Inverted	enlarged
Converging Lens $f > 0$	$s > 2f$	$f < s' < 2f$, real	inverted	enlarged
Converging Lens $f > 0$	$s = f$	∞	?	enlarged
Converging Lens $f > 0$	$s = \infty$	$s' = f$, real	inverted	"tiny"
Diverging Lens $f < 0$	anywhere	$s' < 0$, virtual	upright	reduced
Diverging Lens $f < 0$	$s = \infty$	$s' = -\lvert f \rfloor$ virtual	upright	"tiny"

2.6.1 Refractive index

The density of an object will affect the refractive index when light penetrates the object [39]. The basic idea is to determine the refractive index of a liquid by calculating the relation of Fresnel reflection data from the fiber–air and fiber–liquid boundaries [40.41]. The temperature can also affect the refractive index, but it is not considered in this system [34, 41, 42]. Other than that, the transmission coefficients of the structure can be very sensitive to small shifts in the situation, which can adjustment either the index or the absorption around (and, particularly, adjacent to) the slab area [40, 41]. The refractive index can also be applied right away to identify the purity of some elements in alimentary control [43]. The magnetic flux intensity has a direct and considerable effect on the refractive index [2]. The density can make the divergent of light after the material have different if the selection of the material of the lens is not right.

The light beam passes through the entire cell uniformly in the wavelength region with high transmittance over the sample, but the bigger fault measurement in the wavelength section, through low transmittance above the sample because the fault is affected by the flatness of the prism surfaces, then the light rays cannot go through but in the neighborhood of the apex angle [40]. A previous study showed that all material has refractive index will be infecting when something phantom on the lens [43]. The focal length (F) of the plano-convex GRIN lens through on the be amalgamated impact of the GRIN and the lens curvature [44].

$$n = \frac{d - r_2 d/(\Delta R - d)}{d + r_2} = \frac{d\Delta R - d^2 - r_2 d}{(d + r_2)(\Delta R - d)} \tag{3}$$

Apart from Equation (2), Equation (3) revealed that if a phantom point-source lies at the lens front vertex, by measuring the lens thickness (d), the refractive index of lens can be estimated, the radius of curvature of the back surface (2r), and the distance between the phantom point and its image point (ΔR) [44]. Because there is no thin-lens estimate in the derivation process, both thick and thin lenses might be examined in this way (the only exception is for a lens with 2r = − d, where Eq. (5) cannot be practical since 2d + r = 0) [44]. Metamaterials can generally be engineered to exhibit electromagnetic characteristics that cannot be found in nature or its constituent components [4, 26, 44].

A positive lens reasons the occurrence laser emission to converge at a focal plane on the transmission cross of the lens, forming a real focus line, while a negative lens causes the occurrence laser emission to emerge from the lens as though it were emanating from a virtual focal plane on the incident side of the lens [26]. For example, a positive lens for RCP (Lens B type) by a focal length of 60 mm designed on 810 nm is Manufacturing and properties for scanning [26]. Figure 9 shows the light field before and after the lens. The placement of the focal point happens because of the shape of the lens itself. Normally a convex lens shows a positive lens and a concave lens as above a negative lens. As shown in figure 9 the conclusion for negative and positive lenses is dependent on the lens and is closely related to the refractive index.

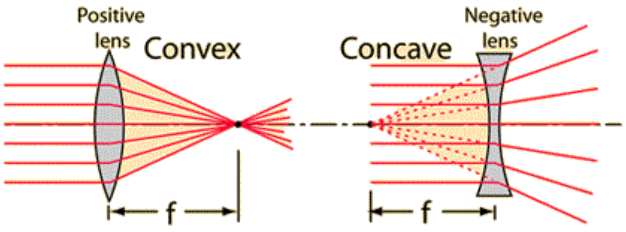

Figure 9 : The negative and positive lens

3.0 Conclusion

According to previous researchers, fan beam technique gives better performance in comparison to parallel beam [15,16,17]. Parallel beam give a limited number of measurement and this will lower the resolution. To improve the performance of the parallel beam projection, the combination between fan beam and parallel beam [28]. This configuration had been proven to improve the resolution. However, in terms of speed, the reputation is lower due to many measurements that have to be counted. Therefore, the solution is choosing the sensor that has a good response. In terms of sensor selection, the majority of the researchers used optoelectronic device because it is easier to handle than the fiber optics. Laser diode is preferred because of its collimation factor and narrower beam of light. Meanwhile, infrared emitter is chosen because of its safety features towards human eyes in comparison to laser. Three methods that can influence the collimation of light, which were; first the sensor to be used must have a small view angle [12,13,14]. Second, no divergence of light between adjacent sensors should occur; the stopper or aperture must be located in front of the sensors. Third, the alternate arrangements between transmitters and receivers can avoid the light from overlapping with each other. The selection of sensors must meet up certain criteria such as low cost, small physical size, luminous intensity, high setting time, high transient characteristics, projection angle and wavelength must also be taken into consideration [1].

The important part in this topic is the lens is available in the market and how to choose the lens by refer the properties or lens.

REFERENCES

[1] R. Abdul Rahim, K.S. Chan, J.F. Pang, L.C. Leong. A hardware development for optical tomography system using switch mode fan beam projection. *Elsevier*, 2005. 277–290.

[2] Dr. Sawsan Ahmed Elhouri Ahmed and Prof. Mubarak Dirar Abd-Alla. The Effect of Magnetic Flux on Newton's Ring Using Typical Glass Lenses with Refractive Index of 1.5. *Journal of Applied and Industrial Sciences*, 2013. 21-29.

[3] G. W. Faris and R. L. Byer, "Beam-deflection optical tomography, *Optics Letters,* 1987. 72 - 75.

[4] Crozier, Kenneth B., Fletcher, D. A., Kino, Gordon S. and Quate, Calvin F.. Micromachined silicon nitride solid immersion lens, *Microelectromechanical Systems, Journal of,* 2002. 470-478.

[5] Siti Zarina Mohd Muji, Ruzairi Abdul Rahim, David A. Johnson, Mohd Hafiz Fazalul Rahiman, Elmy Johana Mohamad, Hudabiyah Arshad Amani and Mohd Fadzli Abdul Sahib. Optical Tomography : Transmitter And Receiver Circuit Preparation, *Jurnal Teknologi Universiti Teknologi Malaysia,* 2011. 13-22.

[6] S. A. Walker, *et al.*, "Image reconstruction by backprojection from frequency-domain optical measurements in highly scattering media, *Applied optics,* 1997. 170 - 179.

[7] E. J. Mohamad. Flame Imaging using Laser Based Transmission Tomography, *Sensors and Actuators A: Physical,* 2006. 332-339.

[8] E. J. Mohamad, Flame Imaging using Laser Based Transmission Tomography, Master Engineering, Universiti Teknologi Malaysia, 2005.

[9] N. Zeng, Lai, S. and Liao, Y. . Optical tomography for two phase flow measurement, *Proceedings of SPIE - The International Society for Optical Engineering,* 2001. 341-347.

[10] P. Dugdale, Green, R.G., Hartley, A.J., Jackson, R.G. and Landauro, J. . Optical Sensors for Process Tomography, *ECAPT. Manchester,* 1992. 26-29.

[11] S. Ibrahim. Measurement of Gas Bubbles in a Vertical Water Column using Optical Tomography, Doctor Philosophy, Sheffield Hallam University, 2000.

[12] J. F. Pang. Real-Time Velocity and Mass Flow Rate Measurement using Optical Tomography, Master Engineering, Universiti Teknologi Malaysia, Skudai, 2004.

[13] K. T. Chiam. Embedded System based Solid-Gas Mass Flow rate Meter using Optical Tomography, Master Engineering, Universiti Teknologi Malaysia, 2006.

[14] C. L. Goh. Real-Time Solids Mass Flow Rate Measurement Via Ethernet Based Optical Tomography System, Master Engineering, Universiti Teknologi Malaysia, 2005

[15] Chan Kok San. Real Time Image Reconstruction For Fan Beam Optical Tomography System," Master Engineering. , Universiti Teknologi Malaysia, 2002.

[16] Chen, Ji, Hou, Dibo, Zhang, Tongjun and Zhou, Zekui. Near infrared laser computed tomography test–system design and application, *Flow Measurement and Instrumentation,* 2005. 321-325.

[17] Lai Chen Leong. Implementation of multiple fan beam projection technique in optical fibre process process tomography, Master Engineering, Universiti Teknologi Malaysia, Skudai., 2005.

[18] R. M. Zain. The Development of a Dual Modality Tomography (DMT) System using Optical and Capacitance Sensors for Solid/Gas Flow Measurement. Master Engineering, Universiti Teknologi Malaysia, 2009.

[19] Ruzairi Abdul Rahim, Chiam Kok Thiam, Jaysuman Pusppanathan and Yvette Shaan-Li Susiapan. Embedded system based optical tomography: the concentration profile," *Sensor Review,* 2009. 54-62.

[20] Guang-xin, Zhang, Ji, Chen and Ze-kui, Zhou. Terahertz PT technology for measurement of multiphase flow and its infrared simulation, *Journal of Zhejiang University Science A,* 2005. 1435-1440.

[21] Zheng, Yingna, Liu, Qiang, Li, Yang and Gindy, Nabil. Investigation on concentration distribution and mass flow rate measurement for gravity chute conveyor by optical tomography system, *Measurement,* 2006. 643-654.

[22] R. Abdul Rahim. A tomography imaging system for pneumatic conveyors using optical fibres, Doctor Philosophy, Sheffield Hallam University, 1996.

[23] G. Held, *Introduction to Light Emitting Diode Technology and Applications*. United State: CRC Press Taylor and Francis Group, 2008.

[24] Chen, Aaron, Yang, Yi, Alqasemi, Umar, Aguirre, Andres and Zhu, Quing. A low cost multi-wavelength tomography system based on LED sources, 2011. 789613-789613-6.

[25] R. R. Mariusz and P. Andrzej. Application of optical tomography for measurements of aeration parameters in large water tanks, *Measurement Science and Technology,* 2003. 199.

[26] Chen, Xianzhong, Huang, Lingling, Mühlenbernd, Holger, Li, Guixin, Bai, Benfeng, Tan, Qiaofeng, Jin, Guofan, Qiu, Cheng-Wei, Zhang, Shuang and Zentgraf, Thomas. Dual-polarity plasmonic metalens for visible light, *Nat Commun,* 2012. 1198.

[27] M. R. Rząsa, The measuring method for tests of horizontal two-phase gas–liquid flows, using optical and capacitance tomography, *Nuclear Engineering and Design,* 2009. 699-707.

[28] C. E. Campbell. The Minimum Distance Between Surfaces Of A Lens At A Point On One Surface, *Journal of the British Contact Lens Association,,* 1995. 3-5.

[29] G. A. Madhugiri and S. R. Karale. High solar energy concentration with a Fresnel lens: A Review, *International Journal of Modern Engineering Research (IJMER),* 2012. 1381-1385.

[30] A. Wehr and U. Lohr. Airborne laser scanning—an introduction and overview, *ISPRS Journal of Photogrammetry and Remote Sensing,* 1999. 68-82.

[31] J. Pendry, Perfect cylindrical lenses, *Optics Express,* 2003. 755-760.

[32] Tony Hough, Ami Livnat and Eliezer Keren. Inter-Laboratory Reproducibility Of Power Measurement Of Topic Hydrogel Lenses Using The Focimeter And The M Oirt Deflectometer, *Journal of the British Contact Lens Association,* 1996. 117-127.

[33] C. E. Campbell. Variation In Lens Thickness As A Function Of Power And Radial Distance From Optical Centre, *Journal of the British Contact Lens Association,* 1995. 127 - 128.

[34] C. E. Jones and J. M. Pope. Measuring optical properties of an eye lens using magnetic resonance imaging, *Elsevier,* 2004. 211 - 220.

[35] X. Zhang and Z. Liu. Superlenses to overcome the diffraction limit, 2008.

[36] Y roja ramani, Sandipan dasgupta, Amrit panda, Supriya pradhan and Bhaskar mazumder. Effect of statins on normal and glucose induced cataract in goat lens, *International Journal of Pharmacy and Pharmaceutical Sciences,* 2012.

[37] M.S. Moghaddam, P. Anil Kumar, G. Bhanuprakash Reddy and V.S. Gholea. Effect of Diabecon on sugar-induced lens opacity in organ culture: mechanism of action, *Elsevier,* 2005. 397–403, 2005.

[38] Bo Tao, Lianguan Shen, Allen Yi, Mujun Li and Jian Zhou. Reducing Refractive Index Variations in Compression Molded Lenses by Annealing, *OPJ,* 2013. 118-121.

[39] Huafeng Ding, Jun Q Lu, William A Wooden, Peter J Kragel and Xin-Hua Hu. Refractive indices of human skin tissues at eight wavelengths and estimated dispersion relations between 300 and 1600 nm, *IOP science,* 2006. 1479-1489.

[40] M. Daimon and A. Masumura. Measurement of the refractive index of distilled water from the near-infrared region to the ultraviolet region, *Applied optics,* 2007. 3811-3820.

[41] C.-B. Kim and C. B. Su. Measurement of the refractive index of liquids at 1.3 and 1.5 micron using a fibre optic Fresnel ratio meter, *IOP,* 2004. 1683-1686.

[42] Min K. Yang, Simon G. Kaplan, Roger H. French and John H. Burnett. Index of refraction of high-index lithographic immersion fluids and its variability, *MOEMS Mems Moems,* 2009. 023005-1 - 023005-6.

[43] H. T. Y. Jin, 1* A. Hiltner,1 E. Baer,1 James S. Shirk. New Class of Bioinspired Lenses with a Gradient Refractive Index, *Wiley InterScience,* 2007. 1834–184.

[44] Lingfeng Chen, Xiaofei Guo and Jinjian Hao. Lens refractive index measurement based on fiber point-diffraction longitudinal interferometry, *Optical Express,* 2013.